

Acute, Lethal, Natural Killer Cell-Resistant Myeloproliferative Disease Induced by Polyomavirus in Severe Combined Immunodeficient Mice

Eva Szomolanyi-Tsuda,* Patricia L. Dundon,*
Isabelle Joris,* Leonard D. Shultz,†
Bruce A. Woda,* and Raymond M. Welsh*

From the Department of Pathology,* University of
Massachusetts Medical Center, Worcester, Massachusetts,
and The Jackson Laboratory,† Bar Harbor, Maine

Infection of severe combined immunodeficient mice, which lack T and B lymphocytes, with polyomavirus (PyV) induced an acute hematological disorder leading to the death of the mice by 2 weeks postinfection. The disease was characterized by a dramatic decrease in megakaryocytes, multiple hemorrhages, anemia, thrombocytopenia, splenomegaly, a massive myeloproliferation and splenic erythroproliferation with a defect in maturation of the myeloid elements similar to that in acute leukemia. This pathology in severe combined immunodeficient mice is very different from that of the well-characterized tumor profiles induced by PyV in normal newborn or nude mice. Viral T and capsid (VP1) antigens and viral genome were detected in some cells in the spleen, but not in the majority of the proliferating myeloid cells. This suggests that the myeloproliferation is induced by some indirect mechanism, such as secretion of growth factors or cytokines by virus-infected cells, rather than by direct transformation by PyV. Neither the spread of PyV, its replication in different organs, nor the pathogenesis or the time of death were altered by depleting natural killer cells in vivo by anti-natural killer cell antibodies. Analysis of the spleen leukocyte population indicated that the cells expressed high levels of class I major histocompatibility complex antigens and were resistant to lysis by activated natural killer cells. (Am J Pathol 1994, 144:359–371)

The dramatic increase in tumor incidence in immunodeficient patients provides evidence for the impor-

tance of immune surveillance in preventing tumor development. Epidemiological data show high frequencies of malignancies in genetically immunodeficient patients, in people receiving immunosuppressive therapy, or in patients with acquired immune deficiency syndrome (AIDS).^{1,2} Interestingly, the predominant tumors observed in immunodeficient people are of a different spectrum than those in the general population and are mainly tumors of the skin, Kaposi sarcomas, or hematological malignancies, such as lymphomas and leukemias. Other characteristic features of these opportunistic tumors are marked aggressiveness and a tendency for quick dissemination. Although some lymphomas are associated with Epstein-Barr virus, the etiology of the overwhelming majority of tumors and leukemias is unknown.³ In this report we show that, in mice homozygous for the severe combined immune deficiency (*scid*) mutation (hereafter referred to as SCID), polyomavirus (PyV) infection causes an acute hematological disorder resembling a malignancy. This pathology is very different from that of the well-characterized tumor spectrum induced by PyV in normal newborn or adult nude mice, and this phenomenon may thus be similar in many ways to the opportunistic tumors discussed above.

PyV infection of mice is an excellent model to analyze the role of the immune system in oncogenesis. Whereas immunocompetent mice infected as adults are resistant to tumor induction, newborn mice infected with PyV develop a wide variety of tumors of mesenchymal and epithelial origin.⁴ In adult athymic nude mice, a more narrow spectrum of tumors is induced, ie, mammary adenocarcinomas with close to 100% incidence and short latency in females and mainly osteosarcomas in males.^{5,6} Transfer of sple-

Supported by grants AI17672, CA34461 (to RMW), AI30389 (to LDS), JDF 192019 (to BAW), and DK 32520 (to IJ).

Accepted for publication October 18, 1993.

Address reprint requests to Dr. Eva Szomolanyi-Tsuda, Department of Pathology, University of Massachusetts Medical Center, 55 Lake Avenue North, Worcester, MA 01655.

nocytes from adult immunocompetent mice immunized with PyV into PyV-infected female nude mice prevented the development of mammary tumors and arrested the growth of one already established tumor, demonstrating the importance of T cells in this system.⁶

Our present study was designed initially to investigate the role of natural killer (NK) cells in the antiviral and anti-tumor host response to PyV. The pathogenesis of PyV infection was examined in SCID mice and in SCID mice pretreated with antibodies that depleted NK cells *in vivo*. Although SCID mice lack functional T and B cells,⁷ they have a normal NK cell response.^{8,9} To our surprise, PyV infection in SCID mice led to a very rapid, lethal disease associated with a myeloproliferation that was not influenced by NK cells. The experiments reported here raise important questions on the pathogenic mechanism of virus-induced neoplasia in immunodeficient hosts and on the contribution of different components of the immune system to the resistance to tumor development.

Materials and Methods

Mice and Virus Inoculations

The newly developed C57BL/6JSz *scid/scid* mice, which were created by continual backcrossing of the *scid* mutation onto the C57BL/6J background for 12 generations, were bred in a research colony at The Jackson Laboratory (Bar Harbor, ME) and shipped when 4 to 6 weeks old to the University of Massachusetts Medical Center. C.B17 *scid/scid* mice were bred and maintained in microisolator cages in the Department of Animal Medicine at the University of Massachusetts Medical Center and were used when 4 to 6 weeks old. The mice were inoculated intraperitoneally with 2×10^5 to 2×10^6 50% tissue culture infectious dose (TCID₅₀) PyV strain A2 (kindly provided by Dr. Michele M. Fluck). The infected animals were euthanized at various times postinfection by cervical dislocation and necropsied. Spleen, liver, lung, bone marrow, and kidney tissues, as well as other organs showing gross abnormality, were fixed in 10% buffered formalin for histology. Spleen samples were frozen in Tissue-Tek optimal cutting temperature compound (OCT, Miles, Inc., Elkhardt, IN) for immunohistochemistry, and samples from different organs were taken for DNA preparations.

NK Cell Depletion *in Vivo*

To deplete NK cell activity, C57BL/6JSz *scid/scid* mice, which express the alloantigen NK1.1, were injected intraperitoneally with 100 μ l of a previously determined optimal dilution of an ammonium sulfate cut of an ascites preparation of a monoclonal antibody to NK1.1¹⁰, or with 20 μ g of an ammonium sulfate cut of another preparation of the same monoclonal antibody. C.B17 *scid/scid* mice, which do not express the NK1.1 alloantigen, received an intraperitoneal injection of 10 μ l of antiserum to asialo GM1 (Wako Chemicals USA, Dallas, TX). The anti-NK1.1 or asialo GM1 injections were repeated weekly. The effectiveness of NK cell depletion was tested in every experiment at day 6 or 7 postinfection by using spleen cells from three to four mice per group in cytotoxicity assays with conventional NK target cells (YAC-1) *in vitro*.

Histopathology and Immunocytochemistry

Formalin-fixed tissues embedded in paraffin were sectioned and stained in standard Harris hematoxylin and eosin. Alternatively a naphthol chloroacetate stain was performed to identify cells of myeloid origin.¹¹ Smears of peripheral blood were stained with Wright-Giemsa. For immunocytochemistry, frozen, OCT-embedded blocks were cut into 5- μ sections, fixed in acetone, and stained with the peroxidase-anti-peroxidase procedure (DAKO Co. Carpinteria, CA), using either rabbit anti-PyV VP1 or brown Norwegian rat anti-PyV small, middle, and large T antigen-specific primary antiserum (generous gifts from Dr. Tom L. Benjamin). The slides were counterstained with hematoxylin.

Electron Microscopy

The spleen was excised, immediately transferred into 3% glutaraldehyde in 0.1 mol/L cacodylate buffer, and rapidly trimmed into 1-mm³ blocks. The latter were further fixed for a total of 5 hours, washed in cacodylate buffer, and postfixed in 2% osmium tetroxide in cacodylate buffer. After rinsing in maleate buffer, the specimens were stained en bloc with 1.5% uranyl acetate in maleate buffer, dehydrated in graded alcohols, and embedded in Epon. One-micron-thick sections were cut to identify the area of interest; thin sections were cut on an LKB Ultratome Nova, stained with uranyl acetate and lead citrate, and examined with a Philips 301 electron microscope.

Virus Titration

PyV strain A2 stocks were grown on NIH 3T3 cells. The virus titers were assayed by serial dilutions on UC1-B cells (murine whole embryo fibroblasts obtained from the American Type Culture Collection) and expressed as TCID₅₀. The recovery of infectious virus from spleens and kidneys removed from mice at day 7 postinfection was done by homogenizing the organs in serum-free Dulbecco's minimum essential medium, incubating them with 0.1 mg/ml collagenase at 37 C for 30 minutes, and then with 0.1 mg/ml elastase for an additional 30 minutes. The homogenates were then frozen and thawed three times to free the virus, centrifuged to remove cell debris, and the supernatant was used for virus titration.

Southern Blots

DNA was prepared from frozen organs (liver, lung, kidney, spleen) following published protocols.¹² Two to 10 µg of undigested DNA or DNA cut with *EcoRI*, which cuts once and therefore linearizes PyV strain A2 genome, was subjected to electrophoresis on 0.8% agarose gels, transferred to nitrocellulose paper by vacuum blotting,¹³ baked, prehybridized, hybridized, washed, and exposed to autoradiography as described.¹⁴ PyV strain A2 cloned in pAT153 plasmid was kindly provided by Dr. Michele M. Fluck, and it was ³²P-labeled by random priming for use as a hybridization probe.

Flow Cytometry Analysis

The following primary antibodies were used for the characterization of spleen cells of infected and uninfected SCID mice: goat anti-mouse immunoglobulin G (IgG), fluorescein isothiocyanate-conjugated (Jackson Immuno Research, Westgrove, PA); rat anti-mouse Thy1.2 (J1J) IgM; J11d, a rat anti-mouse IgG₁ recognizing a B cell and granulocyte marker; CZ1, a rat anti-mouse IgM detecting a sialated modification of CD45RB¹⁵; rat anti-mouse class II IgG_{2b}; rat anti-mouse class I IgG_{2a} (obtained from the American Type Culture Collection); and rat anti-mouse Mac-1 IgG_{2b} phycoerythrin conjugate (Boehringer Mannheim Corp., Indianapolis, IN). Fluorescein isothiocyanate-conjugated goat anti-mouse or goat anti-rat IgG (Fisher Scientific, Malvern, PA) was used as a second antibody, when necessary. Five × 10⁵ to 10⁶ cells were first incubated with normal mouse serum (1:10 dilution) and then stained with the reagents, followed by fixing with

1.1% paraformaldehyde before analysis by flow cytometry using a Beckton Dickinson Flow Cytometer.

Cytotoxicity Assays

A standard microcytotoxicity assay with spleen leukocyte effector cells was used with ⁵¹chromium-labeled YAC-1, L929, or spleen leukocyte targets in quadruplicates with four to five different effector to target cell ratios.¹⁶ The assays were run for 4 hours.

Results

Mortality of PyV-Infected SCID Mice

Figure 1 shows the survival curves of 47 C57BL/6 SCID and 18 C.B17 SCID mice injected intraperitoneally with 2 × 10⁵ to 2 × 10⁶ TCID₅₀ PyV strain A2. All of the inoculated animals died by day 16 postinfection. There was no appreciable difference between the survival time of mice with or without NK cell depletion (mean survival time of C57BL/6 SCID mice 14 days, of C.B17 SCID mice 13.7 days, of NK cell-depleted C57BL/6 SCID mice 13.8 days, and of NK cell-depleted C.B17 SCID mice 14.2 days, respectively). Neither the genetic background (C.B17 or C57BL/6) nor the sex of the mice influenced the survival (Figure 1, A and B). Reduction of the virus dose by five orders of magnitude delayed the time of death by up to 7 days.

Pathology and Histopathology

One to 2 days before death, the mice developed pathological changes, including inactivity, ruffled fur, coolness to touch, weight loss, and multiple hemorrhagic skin lesions (Figure 2A). Analysis of the pathology and histopathology of the animals sacrificed when moribund revealed a complex hematological disorder (Figures 2 and 3). There was a striking splenomegaly, which was more pronounced in C.B17 SCID mice than in C57BL/6 SCID mice. The weight of the spleen from uninfected C57BL/6 SCID mice was 27 ± 3 mg, from day 14 PyV-infected C57BL/6 SCID mice 81 ± 6 mg, from uninfected C.B17 SCID mice 50 ± 6 mg, and from day 14 PyV-infected C.B17 SCID mice 233 ± 47 mg. These values represent the average of the data of four to six mice in each group. Hemorrhagic lesions of the skin, and occasionally of other organs (eg, intestine, liver, etc.) were observed (Figure 2, A and C) and peripheral blood smears at day 14 postinfection indicated a marked thrombocytopenia and

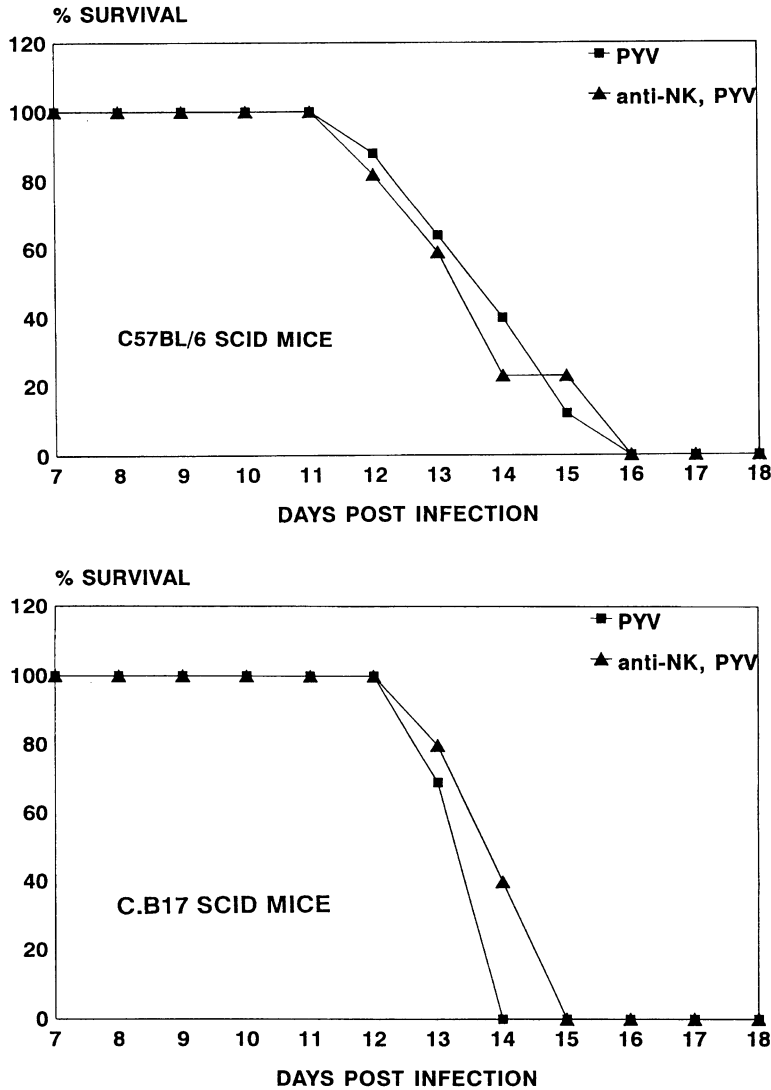


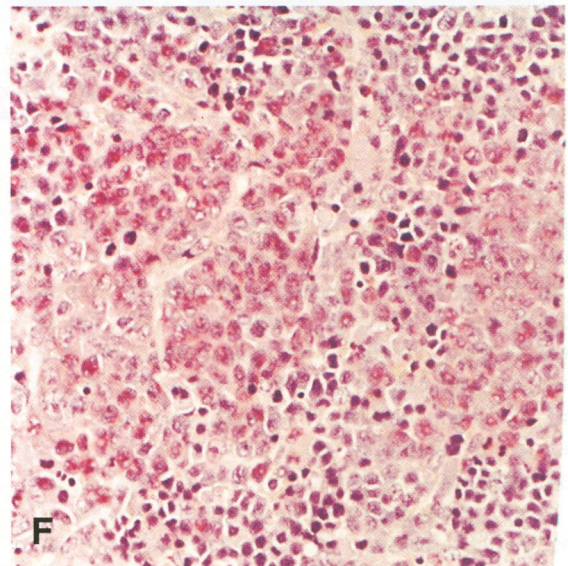
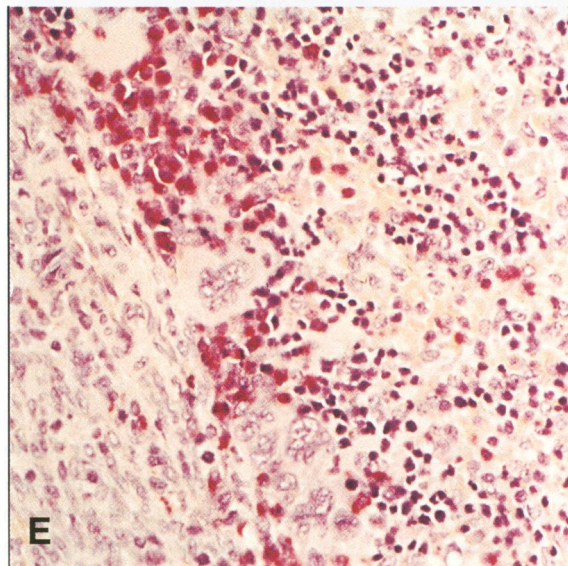
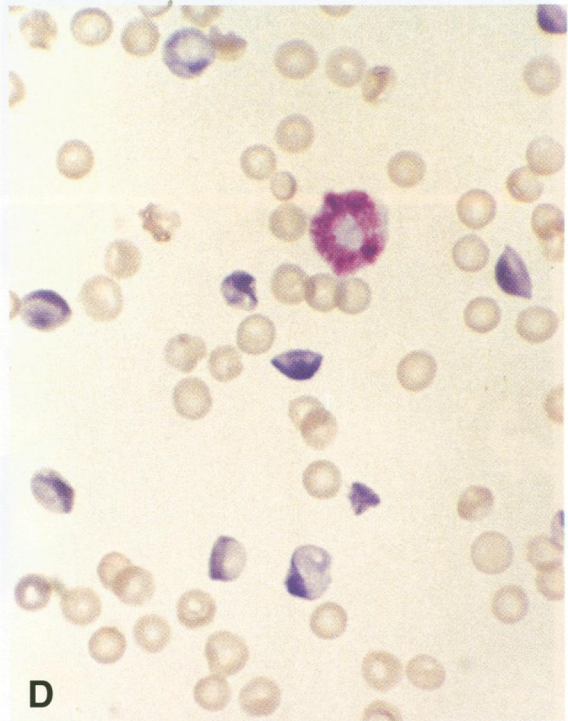
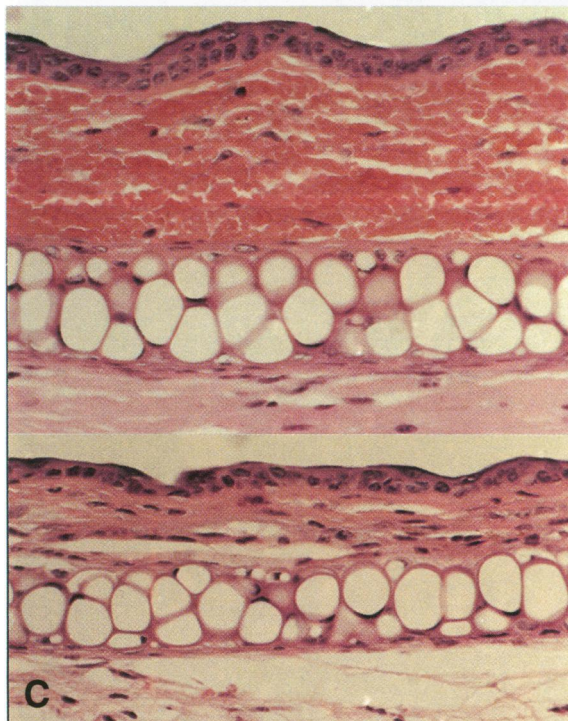
Figure 1. Survival of SCID mice infected with PyV. **A:** C57BL/6 SCID mice (all females) with or without in vivo NK cell depletion were injected intraperitoneally with 2×10^5 to 2×10^6 TCID₅₀ PyV strain A2. PyV-infected mice (n = 25); NK cell-depleted, PyV-infected mice (n = 22). **B:** C.B17 SCID mice (eight males and 10 females) with or without NK cell depletion were injected intraperitoneally with 2×10^5 to 2×10^6 TCID₅₀ PyV strain A2. PyV-infected mice (n = 13); NK cell-depleted, PyV-infected mice (n = 5).

polychromatophilia (Figure 2D), consistent with hemorrhage and compensatory erythropoiesis. The platelet number in peripheral blood samples of day 14 PyV-infected SCID mice was $101,600 \pm 56,600/\mu\text{l}$, whereas in uninfected SCID mice it was $1,570,000 \pm 245,200/\mu\text{l}$ (average values of data obtained from three mice per group).

Histopathological studies of the spleen and bone marrow were performed at 7 and 12 days after infection to determine the morphological effects that

virus infection produced in these organs. Seven days after infection the spleen showed myeloid hyperplasia with an appreciable increase in immature myeloid precursors (left-shifted maturation) (figure not shown). Islands of erythroid precursors remained prominent. Megakaryocytes were reduced in numbers and some showed degenerative nuclear features. The bone marrow was hyperplastic, with reduced megakaryocytic and erythroid activity. Some of the megakaryocytes showed degenerative

Figure 2. Gross and microscopic pathology of PyV-infected SCID mice. **A:** Hemorrhagic skin lesions on the chest 14 days postinfection (approximately 4 \times natural size). **B:** Spleens from PyV-infected (14 days post infection) (top) and uninfected (bottom) C.B.17 SCID mouse (approximately 4 \times natural size). **C:** Histopathology of a skin lesion of the ear of a C57BL SCID mouse 14 days after PyV infection showing hemorrhage spreading throughout the dermis. **Bottom:** another area of the ear with no pathological changes (H&E, 250 \times). **D:** Peripheral blood smear at day 14 postinfection showing polychromatophilia (Wright-Giemsa staining, 900 \times). **E:** Spleen of uninfected SCID mouse, naphthol chloroacetate NCA staining, which stains cells of the myeloid lineage bright red (285 \times). **F:** Spleen at day 12 postinfection, naphthol chloroacetate staining. The number of cells staining red is increased compared to the uninfected spleen, and the pattern of staining is more diffuse, indicating the presence of immature myeloid cells (285 \times).



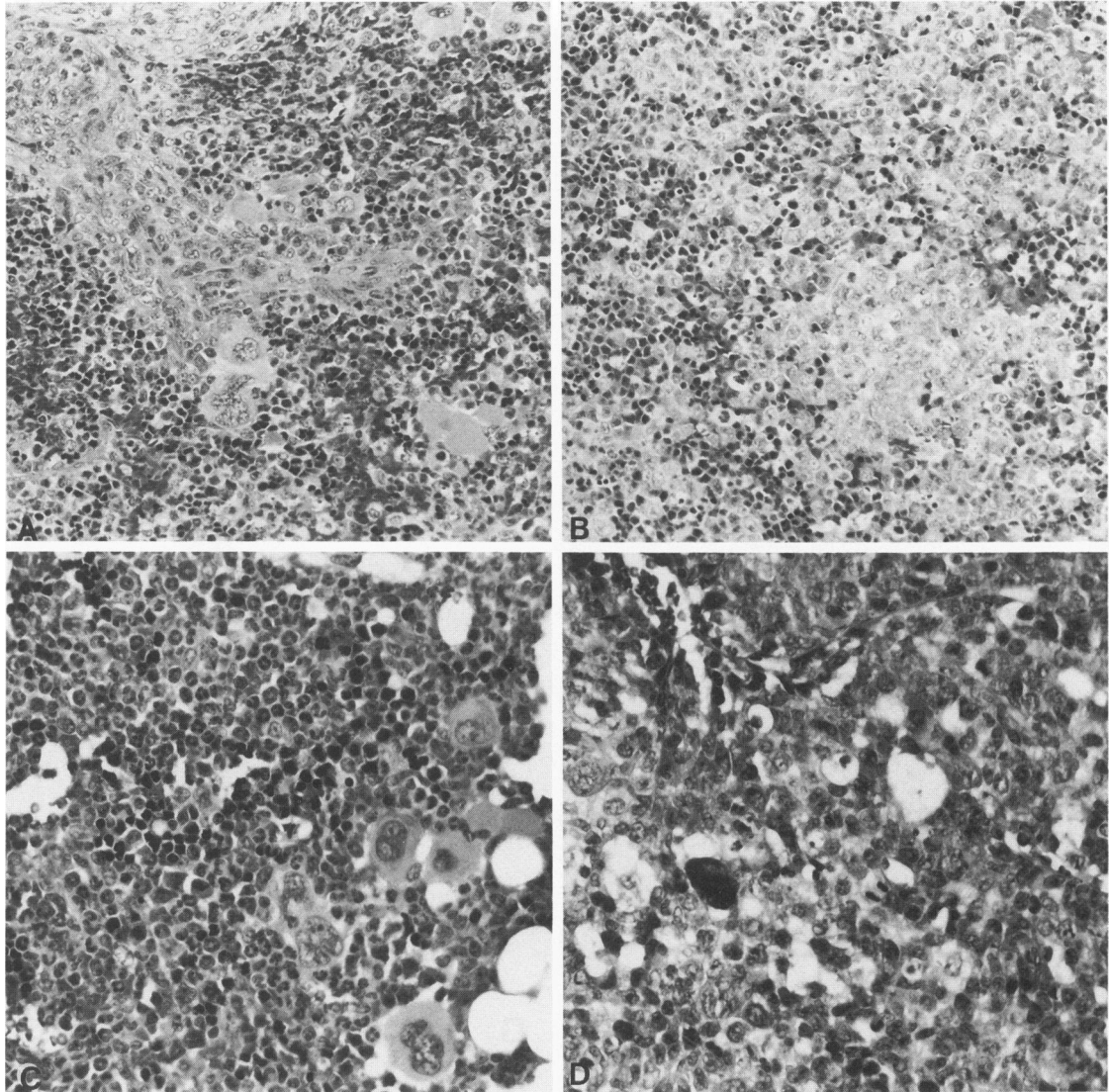


Figure 3. Histopathology of spleen and bone marrow. **A:** Uninfected CB.17 SCID mouse spleen, H&E, 200 \times . **B:** Spleen of PyV-infected CB.17 SCID mouse at day 12 postinfection. The number of megakaryocytes is largely reduced; in the red pulp, large islands of immature myeloid cells are surrounded by erythroid precursors (H&E, 200 \times). **C:** Uninfected CB.17 SCID mouse bone marrow (H&E, 300 \times). **D:** Bone marrow of PyV-infected CB.17 SCID mouse at day 12 postinfection. The highly cellular bone marrow is mainly composed of immature myeloid cells (H&E, 400 \times).

features. The myeloid series was hyperplastic and showed markedly left-shifted maturation.

By 12 days after infection there was a progression in the morphological alterations. The spleen showed large islands of immature myeloid elements within the red pulp (Figure 2, E and F, Figure 3, A and B). These islands of myeloid cells were surrounded by erythroid precursors. Megakaryocytes were reduced in numbers. The bone marrow (Figure 3, C and D) was nearly 100% cellular and was composed predominantly of immature myeloid elements. Morphologically, the extent of this myeloproliferation resembled an acute leukemic process.

Erythroid and megakaryocytic precursors were markedly reduced in numbers.

PyV Replication in SCID Mice

Virus Titers in Kidney and Spleen

Levels of infectious virus recovered from kidneys and spleens of PyV-infected SCID mice at day 7 were measured by serial dilutions on murine embryonic fibroblast cells. Kidneys, in addition to skin, bones, mammary and salivary glands, are major sites of PyV replication in normal mice infected neonatally with

this strain, A2.^{5,17,18} Because the spleens showed many pathological changes in the infected animals (Figure 2, F and G, Figure 3, A and B), homogenates of this organ were also tested for infectious virus. The results obtained in a typical experiment are shown in Table 1. High levels of virus were found in the kidneys, and even higher (three- to 10-fold) in the spleens. This is in contrast to the results obtained in neonatally infected mice with intact immune systems, where the spleens do not support PyV replication.¹⁷ NK cell depletion did not lead to an increase in the virus titers, suggesting that NK cells do not control polyomavirus replication in these organs. This is consistent with the survival curves (Figure 1), which were not influenced by NK cells.

Detection of Viral Genome by Southern Blot Analysis

The spread and replication of PyV in SCID mice was further tested by Southern blot analysis of DNA samples prepared from kidney, spleen, liver, and lung tissues at day 7 and day 14 following infection. As Figure 4 illustrates, at day 7 in all four organs tested, the viral DNA was easily detectable. On blots of gels with DNA samples digested with *EcoRI*, which cuts the circular PyV genome once, the virus-specific signal was observed as a 5.3-kb band, at a position equivalent to that of the linear PyV genome, indicating the presence of nonintegrated PyV in the samples. The amount of polyomavirus genome was estimated to be 20 to 100 copies per cell by comparison to known amounts of cloned viral genomes (data not shown). The relative amount of viral signal in the different organs slightly varied in individual mice. The spleen usually contained the strongest, and the lung the weakest signal.

At day 14 postinfection, all four tissues tested (kidney, liver, lung, and spleen) contained viral signal that showed a slight increase in intensity when compared to day 7 DNA samples. This result sug-

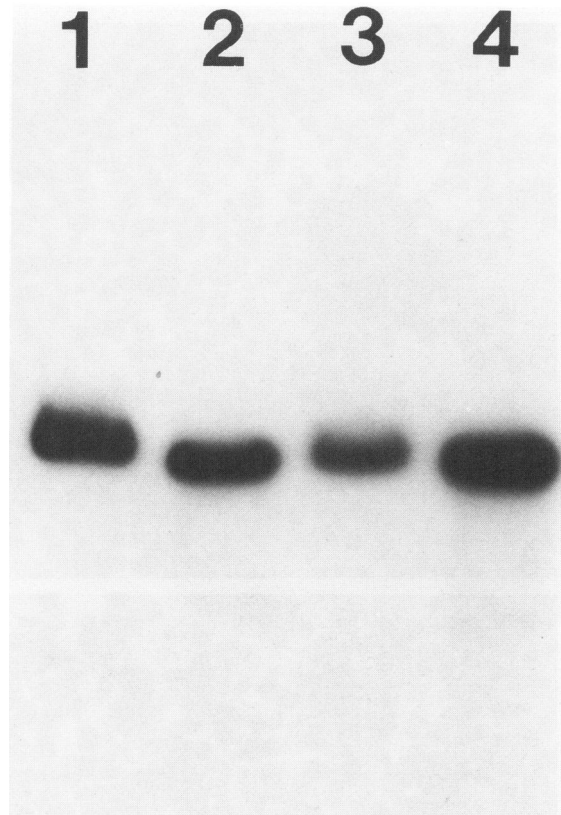


Figure 4. Detection of PyV genome in different organs by Southern blot analysis. Five µg of DNA samples isolated from organs of PyV-infected SCID mice at day 7 postinfection were digested with *EcoRI*. After electrophoresis and transfer, the blots were probed with ³²P-labeled plasmid carrying the PyV genome. Lane 1: kidney, lane 2: liver, lane 3: lung, lane 4: spleen.

gests that SCID mice are unable to clear polyomavirus infection. Consistent with this observation is the detection of viremia. Co-cultivation of peripheral blood samples of PyV-infected mice at day 14 postinfection with UC1b cells, which are permissive for PyV replication, demonstrated the presence of infectious virus in the blood.

Detection of PyV-Infected Cells in the Spleen by Immunohistochemistry and Electron Microscopy

Frozen sections of the spleen were stained for the viral capsid antigen VP1, using rabbit anti-PyV VP1 antibody, and for the T antigens (small, middle, and large), using a rat anti-T antigen antibody, with the peroxidase-anti-peroxidase method at different times following infection. At the earliest time point tested, day 4, megakaryocytes stained positively for the PyV-specific early (Tag) or late (VP1) antigens (Figure 5a). The permissive infection of megakaryocytes 4 days after polyomavirus infection could well

Table 1. PyV Titers of Kidney and Spleen of C57BL SCID Mice 1 Week Post-Infection

Mice	PyV titer	
	TCID ₅₀ /kidney	TCID ₅₀ /spleen
#1Py*	3.0 × 10 ⁶	3.0 × 10 ⁷
#2Py	6.0 × 10 ⁵	8.0 × 10 ⁵
#3Py	3.6 × 10 ⁶	1.6 × 10 ⁷
#4αNKPy†	1.3 × 10 ⁶	8.0 × 10 ⁶
#5αNKPy	1.8 × 10 ⁶	8.0 × 10 ⁷
#6αNKPy	3.6 × 10 ⁶	8.0 × 10 ⁶

* Py₁ mice injected with 5 × 10⁶ TCID₅₀ PyV.
 † αNKPy₁ mice injected with 5 × 10⁶ TCID₅₀ PyV and mAb αNK1.1.

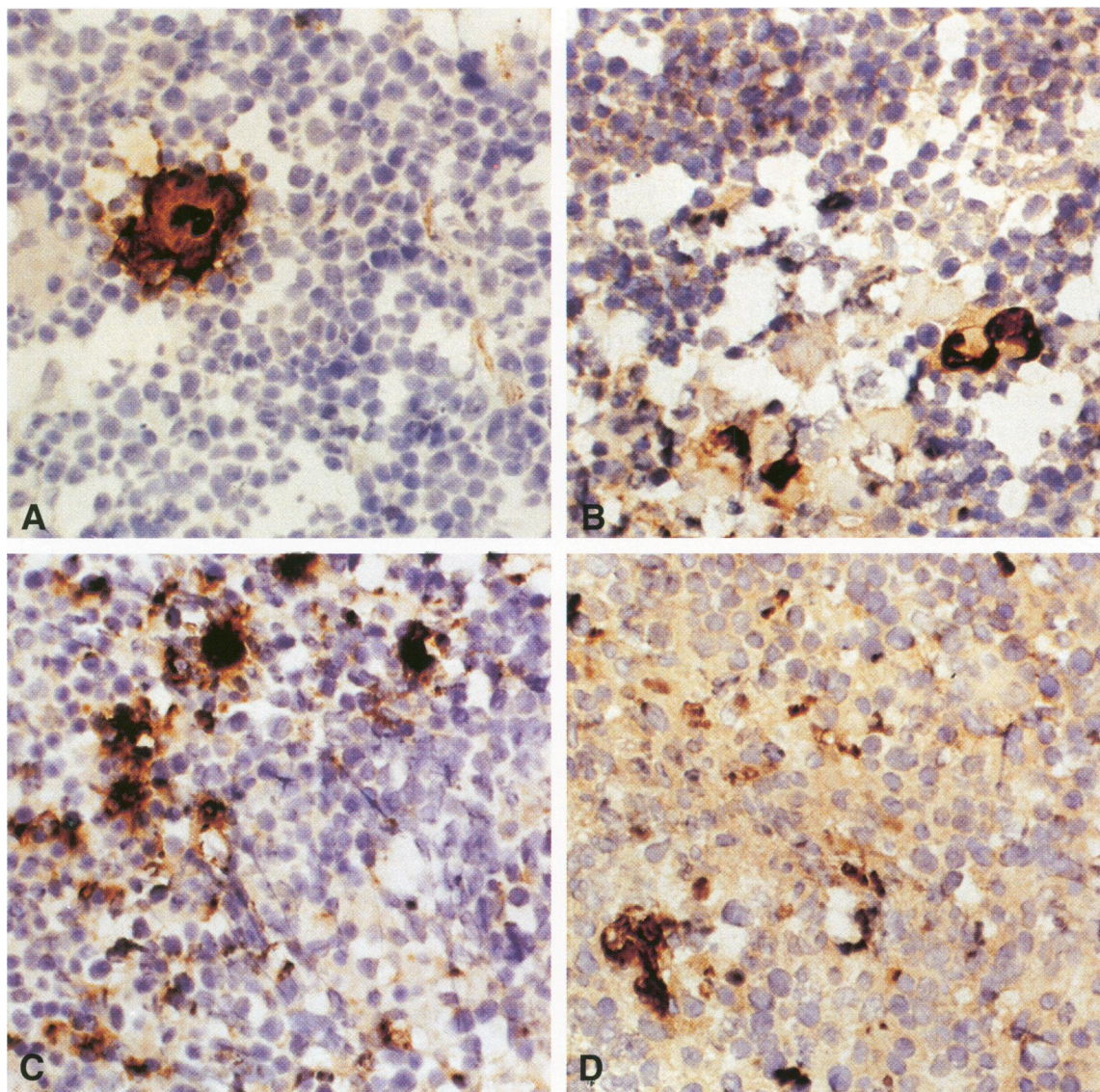


Figure 5. Immunoperoxidase staining of spleen from PyV-infected SCID mice with PyV-specific antibodies. **A:** Spleen at day 4 postinfection, stained with VP1-specific monoclonal antibody, 430 \times . **B:** Spleen at day 4 postinfection, stained with a small, middle, and large T antigen-specific antiserum, 430 \times . **C:** Spleen at day 7 postinfection, stained with VP1-specific monoclonal antibody, 430 \times . **D:** Spleen at day 7 postinfection, stained with small, middle, and large T antigen-specific antiserum, 215 \times .

account for the decrease in megakaryocytes in the spleen and bone marrow by day 7 and for the further decrease in megakaryocytes and subsequent thrombocytopenia by day 14. At day 7, numerous cells stained positively with both the T antigen- and the VP1-specific antibodies (Figure 5b), and by day 14, the number of cells containing viral signal increased slightly. The majority of the spleen cell population, however, did not show detectable staining with the virus-specific reagents even at day 14, and virtually identical results were seen by *in*

situ hybridization methods (data not shown). Therefore, it is likely that the majority of the proliferating immature myeloid cells did not harbor polyomavirus.

Spleen tissues of PyV-infected SCID mice were studied by electron microscopy. At day 14 postinfection, cells in the spleen containing viral particles exhibited cytoplasmic and/or nuclear damage, ranging from mild to severe. These changes included cytoplasmic swelling with or without nuclear pyknosis or lysis; in some cells, the nucleus alone was affected.

Many infected dying or dead cells were loaded with viral particles organized in crystalline arrays. A number of macrophages contained electron-dense phagosomes with viral particles, which either filled the phagosome or lined the inner surface of its membrane. Some immature cells with abundant, normal-looking cytoplasm and a few lysosomelike inclusions were seen to harbor in their nucleus a large number of viral particles (Figure 6), distributed in a pattern reminiscent of chromatin. Another feature of these nuclei was the condensation of the chromatin into one to three large clumps.

Spleen Cells of PyV-Infected SCID Mice Express High Level of Major Histocompatibility Complex (MHC) Class I and Low Level of MHC Class II Antigens

Surface antigens expressed on spleen cells of PyV-infected, PyV-infected and NK cell depleted, and uninfected SCID mice were characterized by fluorescence-activated cell sorter analysis with a panel of monoclonal antibodies. As expected for mice homozygous for the SCID mutation, the splenocytes were mostly Thy1-, IgG-, J11d+, Mac-1+

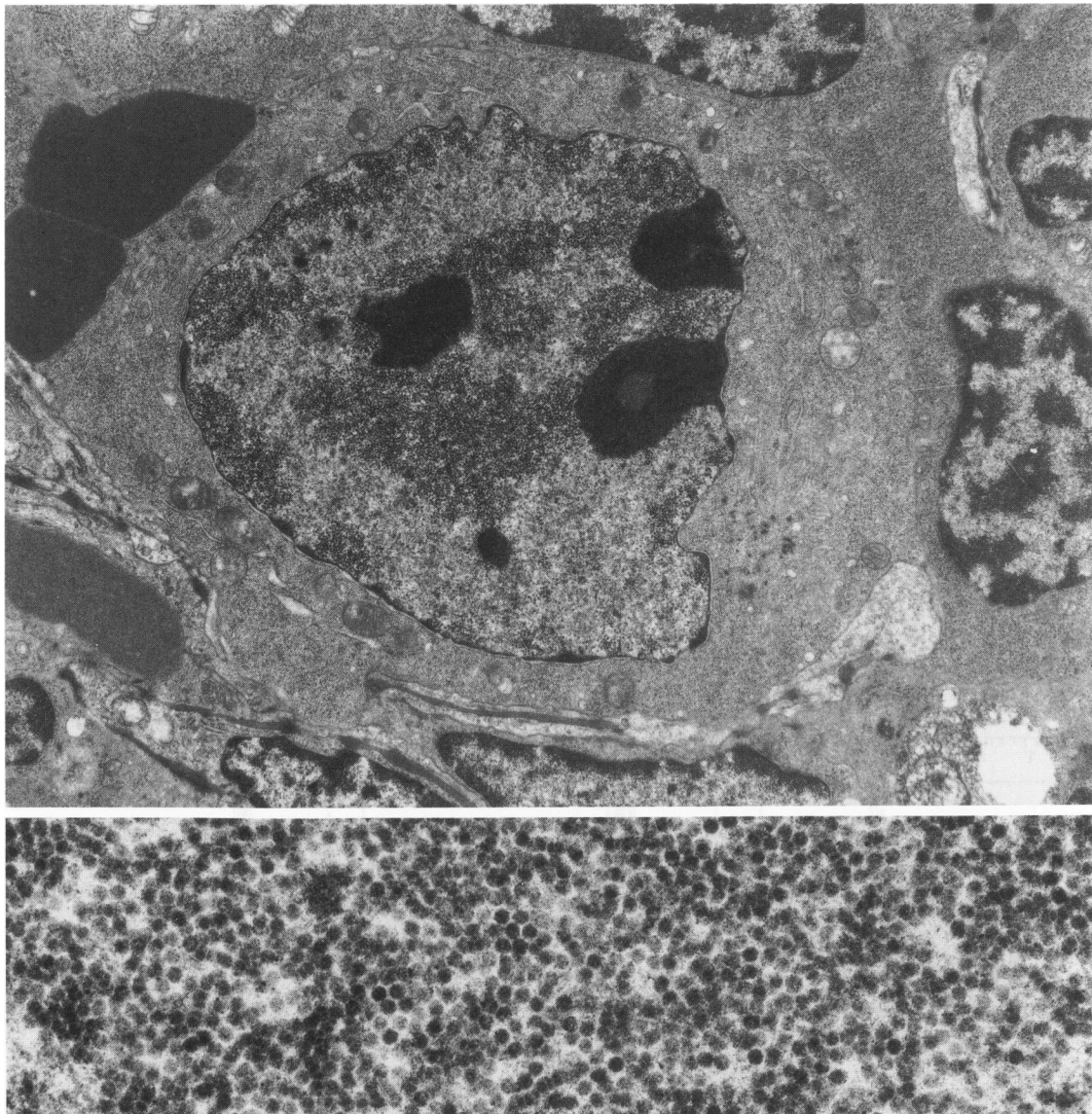


Figure 6. Electron micrographs of a PyV-infected spleen cell from a C.B17 SCID mouse 14 days postinfection. **Top:** Immature cell characterized by abundant cytoplasm and few inclusions. Prominent nucleus with clumps of condensed chromatin and a large number of viral particles (7,140 \times). **Bottom:** higher power picture of the viral particles (diameter 40 nm) located between the two lower clumps of chromatin (51,300 \times).

in all three groups of animals. The most interesting finding was that, whereas spleen cells from uninfected SCID mice displayed low class I and high class II expression, mice 14 days after PyV infection showed very high class I and low class II expression (Figure 7). Expression of the CZ-1 antigen, which detects a sialated form of CD45RB expressed on NK cells, B cells, and most T cells, was very low after PyV infection, indicating the non-lymphoid nature of the cells. NK cell depletion *in vivo* did not influence these changes in class I, class II, and CZ1 expression (data not shown). It is important to note that spleen cells obtained from day 12 to 14 PyV-infected mice consistently had no NK activity *in vitro*. The ^{51}Cr release using YAC-1 target cells at an effector to target ratio of 50, in a 4-hour cytotoxicity assay was 14% with uninfected C57BL/6 SCID mice splenocyte effectors, 44% with splenocytes from day 6 PyV-infected SCID mice, and 3.4% with splenocytes from day 13 PyV-infected SCID mice, showing that there were few functionally active NK cells present at this final stage of the disease and/or that the NK cells were

diluted by the myeloproliferation. The decrease of CZ-1 expression in the spleen cells is consistent with this finding.

Spleen Cells from Polyomavirus-Infected SCID Mice Are Resistant to Killing by Activated NK Cells *in vitro*

Normal splenocytes are usually relatively resistant to NK cell-mediated lysis, but hematopoietic precursor cells and specifically myeloid precursor cells are normally sensitive to regulation by NK cells.¹⁹ High MHC class I expression has been shown to confer resistance to target cells against NK-mediated lysis,²⁰ and therefore we tested whether the high MHC class I-expressing spleen cells from day 14 PyV-infected SCID mice will resist lysis by highly activated NK cells *in vitro*. The sources of highly activated NK cells were spleens from day 3 lymphocytic choriomeningitis virus-(LCMV) infected C.B17 *scid/scid* mice or from day 3 LCMV-infected C3H/HeSnJ mice. These effector cells showed a high level of cytotoxicity against

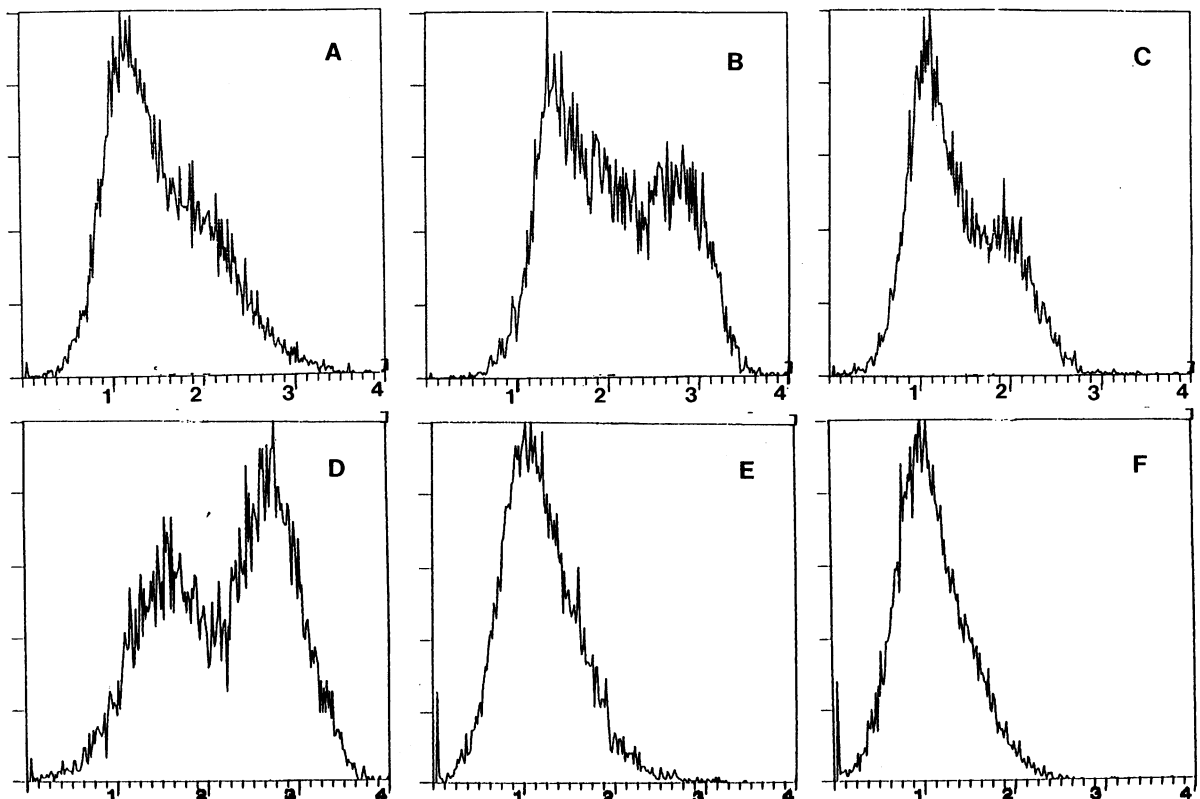


Figure 7. MHC class I, MHC class II, and CZ-1 expression on spleen cells of PyV-infected C.B17 SCID mice. The y axis represents cell number, the x axis log fluorescence intensity. A, B, and C: Spleen cells from uninfected SCID mice; D, E, and F: spleen cells from PyV-infected SCID mice at day 14 postinfection. A and D were stained with anti-class I; B and E with anti-class II; C and F with anti-CZ-1 antibodies.

YAC-1 and L929 target cells, but they did not have any cytotoxic activity against spleen leukocytes harvested from day 14 PyV-infected mice (Figure 8).

Discussion

Our study shows that PyV in SCID mice induces an acute, fatal hematological disorder leading to the death of the mice by 2 weeks postinfection. The disease is characterized by a dramatic decrease in megakaryocytes and platelets, multiple hemorrhages, anemia, and a massive myeloproliferation associated with a defect in maturation of the myeloid elements, which is morphologically very similar to leukemia. This finding is surprising, because the pathology in SCID mice is entirely different from any disease known to be caused by PyV in neonatal and nude mice or in mice transgenic for PyV oncogenes. This result is reminiscent of clinical observations showing a high prevalence of a narrow set of malignancies in immunocompromised patients, whereas in the immunocompetent population these

malignancies are extremely uncommon and different tumors are predominant. The mouse PyV system is easy to manipulate and thereby provides an excellent opportunity to address the important question of how the functioning of different components of the immune system alters disease specificity.

Although productive infection and transformation are thought to be mutually exclusive in the case of DNA tumor viruses, the same cell types that support PyV replication can serve as targets for tumor induction. PyV-induced tumors consist of cells with three different types of infection: cells containing a high number of free viral genomes and expressing VP1 capsid protein (lytically infected cells), cells containing one or few viral genomes—presumably integrated—and expressing no VP1 (corresponding to true transformed cells), and cells having a high copy number of unintegrated genomes, but lacking VP1, suggesting an unusual postreplicational block of viral gene expression.²¹ The regulatory mechanisms operating in these processes are unknown. The high oncogenic potential of some PyV strains shows good correlation with their ability to replicate and spread in different murine target tissues, and these properties map to the VP1 major capsid protein.^{21,22} These data suggest that a high level of virus replication in a given tissue is a prerequisite for efficient tumor induction. The fact that tumors that most frequently arise in neonatally PyV-infected mice are found in the salivary gland, skin, bones, mammary glands—which are predominant sites of virus replication—supports this concept.⁴

In adult immunocompetent mice PyV does not cause pathology and does not reach levels high enough to be detectable by conventional techniques (Southern blots, plaque assays). In newborn mice with intact but immature immune systems, viremia develops by day 3, and the virus replicates in most organs tested, including the skin, bones, and kidney, where peak virus levels are observed at days 7 to 8. After the onset of the antiviral immune response, however, the virus is quickly cleared, with the exception of a low level of persistent infection in the kidney and bone.^{17,18} The pattern of polyomavirus replication is quite different in adult athymic nude mice. There is no viremic phase of the infection, the virus replication is more slow, and it is mainly confined to skin, bone, mammary and salivary glands, and sometimes spleen.¹⁷ Polyomavirus has not been detected in these animals in the kidney, liver, or lung. The narrow set of tumors induced in these mice (mainly mammary adenocarcinomas in females and osteosarcomas in males) can be explained by the restricted replication pattern and by

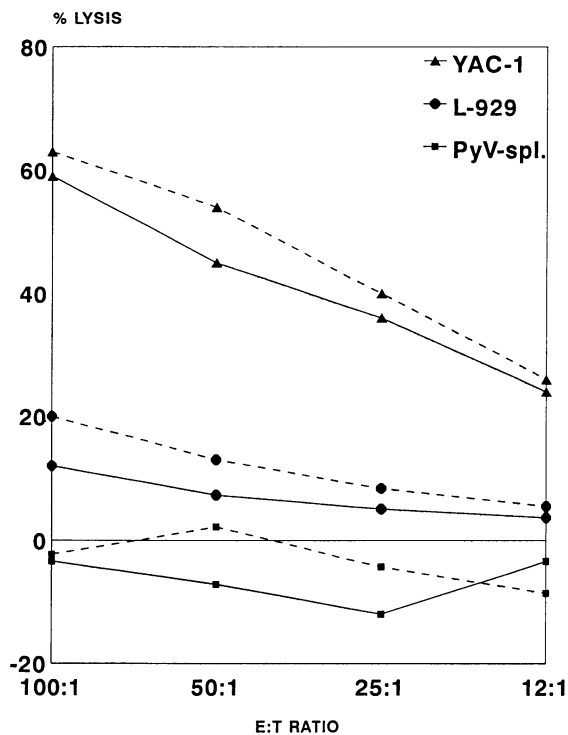


Figure 8. PyV-infected splenocytes are resistant to lysis by highly activated NK cells. Standard 4-hour cytotoxicity assay was performed at different effector to target ratios. Experiment #1 (solid lines) was performed with splenocyte effector cells from LCMV-infected C.B17 SCID mice at day 3 postinfection, using YAC-1 cells, L929 cells, and spleen cells from day 14 PyV-infected C.B17 SCID mice as targets. Experiment #2 (dotted lines) was done with effector spleen cells from LCMV-infected C3H mice at day 3 postinfection, with YAC-1 cells, L929 cells and spleen cells from day 14 PyV-infected SCID mice as targets.

the rapid development of these malignancies leading to the death of the animals before the other, more slowly growing tumors could appear.

Our present study shows that in adult SCID mice, PyV replicates progressively even in organs that do not support virus replication in adult athymic nude mice (kidney, lung, liver). This finding suggests that an immunological mechanism might be responsible for the different patterns of replication.

The acute myeloid cell proliferation in SCID mice described in this report is very surprising because PyV is not known to be associated with hematological malignancies, and, with the exception of Friend leukemia cell lines *in vitro* and macrophages *in vivo*, cells of the hematopoietic system are not known to be infectible with PyV.⁴ The possibility that a retrovirus is activated during the course of the PyV infection and causes leukemia is highly unlikely, as reverse transcriptase assays performed with spleen cell supernatants from day 14 infected mice were negative (data not shown). The experiments reported here clearly show that PyV replicates in the spleen, initially in megakaryocytes and later in other cells as well. However, the data indicate that high levels of VP1, T antigens, or viral genome are not present in the vast majority of the abnormally proliferating cell population. This suggests that the virus induces this disease via a novel, indirect mechanism and not by direct transformation of the cells by PyV oncogenes. A plausible hypothetical mechanism could be the production of cytokines and/or growth factors by PyV-infected cells, which could trigger massive polyclonal proliferation of one or more cell types of the hematopoietic system. The suggestion that PyV-infected cells might be able to trigger malignant cell proliferation by an indirect mechanism has precedent. Dawe et al²³ described in PyV-infected mice the emergence of T-cell lymphomas in close proximity to salivary lymphoepitheliomas; these T lymphomas presumably did not arise as a consequence of direct virus-induced transformation, as the cells did not have any detectable PyV DNA. We hypothesize that indirect mechanisms of tumor induction by viruses may occur in immunocompromised organisms. The growing prevalence of polyclonal lymphomas without *c-myc* rearrangement within the AIDS-associated non-Hodgkin's lymphoma cases, which do not carry Epstein-Barr virus genome, and therefore do not seem to arise as a consequence of "direct" transformation by Epstein-Barr virus,²⁴ seems to support this view.

The very early onset after infection and the highly acute nature of the disease is also surprising. Retro-

virus vectors expressing the PyV middle T (mT) oncogene can cause cavernous hemangiomas starting at 2 to 4 weeks postinfection.^{25,26} Mice transgenic for mT also develop endothelial tumors, or, if mT is linked to mouse mammary tumor virus promoter, multifocal mammary tumors by 3 weeks of age.^{27,28} These data indicate that mT can cause one-step oncogenesis. Acting alone, it has a target specificity for endothelial cells, and when it is expressed in high levels, or when it is present in every cell, as in transgenic animals, the induced malignancies appear quite rapidly. However, in the context of the whole virus there is a much broader tumor spectrum, and longer time is needed for tumor development. Even in nude mice, the earliest tumors appear at about week 6. In PyV-injected SCID mice, massive myeloproliferation can be observed as early as day 7, shortly after the virus replication reaches high levels. This also might indicate that the myeloproliferation is triggered by cell proliferation-promoting substances produced or induced by virus-infected cells rather than by direct transformation by the virus.

Very few studies have been reported so far investigating the function of different components of the immune system in preventing PyV infection or oncogenesis. Experiments published by Wirth and Fluck⁶ provided evidence that T cells have a major role in the protection against polyomavirus-induced oncogenesis. Our study shows that NK cells do not seem to control PyV replication in SCID mice. NK cells also seem to be incapable of effectively responding to or controlling the myeloid cell proliferation in these animals. This conclusion is based on *in vitro* cytotoxicity assays, and on the observation that NK cell depletion does not influence the time course and the severity of the disease. The fact that splenocytes have a large increase in MHC class I antigen expression in polyomavirus-infected SCID mice can be a contributing factor to the inability of activated NK cells to attack these abnormal proliferating cells, as high levels of class I MHC expression can protect target cells from NK cell-mediated lysis. The role of humoral immunity, particularly of the T-cell independent B-cell response, as well as the role of $\gamma\delta$ T cells are not understood in PyV infection.

Acknowledgments

We thank Ms. Yu Liu, Ms. Laura Rooney, Mr. Roger Solomon, and Mr. Lou Savas for their excellent technical assistance; Dr. Tom L. Benjamin for the gift of anti-VP1- and anti-T antigen-specific antibodies; Dr.

Michele M. Fluck for providing us PyV A2 virus stock and PyV A2 DNA cloned in plasmid; and Ms. Jean M. Underwood for help in preparation of figures.

References

1. Filipovich AH, Mathur A, Kamat D, Shapiro RS: Primary immunodeficiencies: genetic factors for lymphoma. *Cancer Res (Suppl)* 1992, 52:5465s–5467s
2. Hoover RN: Lymphoma risks in populations with altered immunity—a search for mechanism. *Cancer Res (Suppl)* 1992, 52:5477s–5478s
3. Ioachim HL: The opportunistic tumors of immune deficiency. *Adv Cancer Res* 1990, 54:301–317
4. Dawe CJ, Freund R, Mandel G, Ballmer-Hofer K, Talmage DA, Benjamin TL: Variations in polyoma virus genotype in relation to tumor induction in mice. *Am J Pathol* 1987, 127:243–261
5. Berebbi M, Dandolo L, Hassoun J, Bernard AM: Specific tissue targeting of polyomavirus oncogenicity in athymic nude mice. *Oncogene* 1988, 2:144–156
6. Wirth JJ, Fluck MM: Immunological elimination of infected cells as the candidate mechanism for tumor protection in polyomavirus-infected mice. *J Virol* 1991, 65:6985–6988
7. Bosma GC, Custer RC, Bosma MJ: A severe combined immunodeficiency mutation in the mouse. *Nature* 1983, 301:527–530
8. Tutt MM, Schuler W, Kuziel WA, Tucker PW, Bennett M, Bosma MJ, Kumar V: T cell receptor genes do not rearrange or express functional transcripts in natural killer cells of scid mice. *J Immunol* 1987, 138:2338–2344
9. Welsh RM, Brubacker JO, Vargas-Cortez M, O'Donnell CL: Natural killer (NK) response to virus infections in mice with severe combined immunodeficiency. The stimulation of NK cells and the NK cell-dependent control of virus infections occur independently of T and B cell function. *J Exp Med* 1991, 173:1053–1063
10. Koo GC, Peppard JR: Establishment of monoclonal anti-NK-1.1 antibody. *Hybridoma* 1984, 3:301–303
11. Higgy KE, Burns GF, Hayhoe FGJ: Discrimination of B, T and null lymphocytes by esterase cytochemistry. *Scand J Hematol* 1977, 18:437–448
12. Sambrook J, Fritsch EF, Maniatis T: *Molecular Cloning: A Laboratory Manual*. Cold Spring Harbor Laboratory, Cold Spring Harbor, New York, 1989
13. Medveczky P, Chang C-W, Oste C, Mulder C: Rapid vacuum-driven transfer of DNA and RNA from gels to solid support. *Biotechniques* 1987, 5:242–246
14. Medveczky P, Szomolanyi E, Desrosiers RC, Mulder C: Classification of herpesvirus saimiri into three groups based on extreme variation in a DNA region required for oncogenicity. *J Virol* 1984, 52:938–944
15. Brutkiewicz RR, O'Donnell CL, Maciaszek JW, Welsh RW, Vargas-Cortez M: The mAb CZ-1 identifies a mouse CD45-associated epitope expressed on IL-2-responsive cells. *Eur J Immunol* 1993, 23:2427–2433
16. Welsh RM: Cytotoxic cells induced during lymphocytic choriomeningitis virus infection of mice. I. Characterization of natural killer cell induction. *J Exp Med* 1978, 148:163–181
17. Wirth JJ, Amalfitano A, Gross R, Oldstone MBA, Fluck MM: Organ- and age-specific replication of polyomavirus in mice. *J Virol* 1992, 66:3278–3286
18. Dubensky TW, Freund R, Dawe CJ, Benjamin TL: Polyomavirus replication in mice: influences of VP1 type and route of inoculation. *J Virol* 1991, 65:342–349
19. Trinchieri G: *Natural killer cells in hematopoiesis. The Natural Killer Cell*. Edited by Lewis CE, McGee JO'D, Oxford University Press, 1992, pp 41–65
20. Karre K: Natural killer cells and the MHC class I pathway of peptide presentation. *Semin Immunol* 1993, 5:127–145
21. Talmage DA, Freund R, Dubensky T, Salcedo M, Gargiolo P, Rangel LM, Dawe CJ, Benjamin TL: Heterogeneity in state and expression of viral DNA in polyoma virus-induced tumors of the mouse. *Virology* 1992, 187:734–747
22. Freund R, Calderone A, Dawe CJ, Benjamin TL: Polyomavirus tumor induction in mice: effects of polymorphisms of VP1 and large T antigen. *J Virol* 1991, 65:335–341
23. Dawe CJ, Freund R, Abromson-Leeman SR, Dubensky TW, Carroll J, Dorf ME, Benjamin TL: T-cell lymphomas emerging as epineoplasms in mice bearing transplanted polyoma virus-induced salivary gland tumors. *Cancer Res (Suppl)* 1990, 50:5643s–5648s
24. Shiramizu B, Herndier B, Meeker T, Kaplan L, McGrath M: Molecular and immunophenotypic characterization of AIDS-associated, Epstein-Barr virus-negative, polyclonal lymphoma. *J Clin Oncol* 1992, 10:383–389
25. Kornbluth S, Cross FR, Harbison M, Hanafusa H: Transformation of chicken embryo fibroblasts and tumor induction by the middle T antigen of polyomavirus carried in an avian retroviral vector. *Mol Cell Biol* 1986, 6:1545–1551
26. Williams RL, Courtneidge SA, Wagner EF: Embryonic lethality and endothelial tumors in chimeric mice expressing polyoma virus middle T oncogene. *Cell* 1988, 52:121–131
27. Bautch VL, Toda S, Hassell JA, Hanahan D: Endothelial cell tumors develop in transgenic mice carrying polyoma virus middle T oncogene. *Cell* 1987, 51:529–538
28. Guy CT, Cardiff RD, Muller WJ: Induction of mammary tumors by expression of polyomavirus middle T oncogene: a transgenic mouse model for metastatic disease. *Mol Cell Biol* 1992, 12:954–961